Kapal: Jurnal Ilmu Pengetahuan dan Teknologi Kelautan
(Kapal: Journal of Marine Science and Technology)
journal homepage : http://ejournal.undip.ac.id/index.php/kapal
2301-9069 (e)
1829-8370 (p)

Hydrodynamic Analysis of High-Speed Vessels in Shallow and Deep Water Using CFD

Budi Utomo[1)], Samuel[2)*)], Parlindungan Manik[2)] , Chiquita Azaria[2)], Syaiful Tambah Putra Ahmad[2)], Zhang Yongxing[3)]

[1)]Marine Construction Engineering Technology, Vocational School, Diponegoro University, Semarang 50275, Indonesia
[2)]Department of Naval Architecture, Faculty of Engineering, Diponegoro University, Semarang 50275, Indonesia
[3)]Nanjing Tianfu Software, Jiulong Lake International Enterprise Park, Jiangning Development Zone, Nanjing, Jiangsu, China

[*)] Corresponding Author : samuel@ft.undip.ac.id

Article Info

Keywords:
Deep Water;
Shallow Water;
Fridsma Hull;
Drag;
CFD;

Article history:
Received: 30/01/2023
Last revised: 03/05/2023
Accepted: 04/05/2023
Available online: 04/05/2023
Published: 14/06/2023

DOI:
https://doi.org/10.14710/kapal.v20i2.52141

Abstract

Differences in the depth of the water surface affect the hydrodynamics of the ship so there is a possibility that the ship will behave differently in deep water and shallow water. The surface flow generated by the hull varies radically due to the speed of the ship and the effects of water depth. At a certain speed, the ship experiences a critical speed condition, which will affect the total resistance of the ship. This study examines the Fridsma ship's resistance to differences in water depth at several speeds. Numerical computation is used in this study to simulate the characteristics of a planing hull form. The Finite Volume Method (FMV) is used to observe fluid flow due to differences in water level with the RANS (Reynolds-Averaged Navier - Stokes) equation in predicting ship resistance. K-ε was modeled as a turbulent and volume of fluid (VOF) model to represent the air and water phases. This study uses a morphing grid mesh to analyze the shape of the hull in numerical simulations. The total resistance of Fridsma in shallow waters increased at each speed when compared to the total resistance in deep waters. On average in deep waters, it can reduce the total resistance by around 22.34% compared to shallow waters. This is caused by the squat phenomenon that occurs in the hull.

1. Introduction

High-speed marine vehicles generally have buoyancy at low speeds, when the ship enters high speeds, the ship's hull will be lifted by hydrodynamic forces to reduce the wetted surface area and resistance [1]. High-speed marine vehicles in their operations require good seakeeping performance and the lowest possible resistance to rough seas [2].

High-speed marine vehicles also use the planing hull concept to increase speed. The shape of the planing hull will increase the hydrodynamic pressure on high-speed marine vehicles to reduce frictional resistance and wave resistance [1]. When operational, planing hull has a concentration on resistance, trim, and heave [3]. Planing hulls vary in their performance in different situations. Therefore, predicting the planing hull performance under different conditions is important. The basic principle of planing hull is the process of generating sufficient hydrodynamic lift on the bottom of the hull to support the weight of the hull [4].

The resistance of high-speed marine vehicles in deep waters has been widely discussed in previous studies. There are differences in resistance in shallow water compared to deep water. When operating in shallow water with subcritical speed (typical for displacement vessels), the speed will slow down with constant power. Conversely, when operating in shallow water with supercritical speeds (typical for planing vessels), the speed of the vessel increases with constant power. In addition, the hull-generated surface waves vary radically with the ship's speed and water depth [5]. In shallow water, the water depth affects the hydrodynamics of the ship. Approaching the critical speed, according to number one Froude depth, a solitary wave is formed in the hull accompanied by fluctuations in lift force [6]. Further to this difference ships may behave differently in shallow water when compared to deep water. In a study conducted by Terziev et al., a strong boundary layer was formed at the bottom of the canal as soon as the ship entered a shallower area. The increase in resistance resulting from a change in depth is approximately up to 226% of the initial value approaching the critical velocity [7].

The purpose of this study was to determine the effect of the water depth on the total resistance of the Fridsma hull form using numerical computational methods. This study uses the Fridsma hull form as an object of angle variation and geometry

variation, as well as validation of the results. Numerical computation is used in this study to simulate the characteristics of a planing hull. Using the finite volume method (FMV) which is based on the RANS equation (Reynolds – Averaged Navier – Stokes). K-ε was modeled as a turbulent and volume of fluid (VOF) model to represent the air and water phases. This study uses a morphing grid mesh to analyze the shape of the hull in numerical simulations [8]. This method further observes the movement and changes of the mesh around the hull, and the hull can move without losing continuity where the hull has a dynamic interaction with the fluid [9].

2. Methods

This research was conducted using the Computational Fluid Dynamics method which is a branch of fluid mechanics where algorithms and numerical methods are used to solve problems related to fluid flow. The CFD program aims to solve equations using the boundary and initial conditions approach.

2.1. Object Research

Material This study uses experimental data from Fridsma in 1969 as a benchmark for results. The experimental data used were trial hulls in still water conditions which can be seen in Table 1 and Figure 1. In this study, five-speed variations were used with Froude Numbers 0.6, 0.9, 1.2, 1.5, and 1.8.

Table 1. Fridsma Experiment Data [10]

Parameter	Unit	Value
L/B	-	5
L	m	1.143
B	m	0.229
T_{AP}	m	0.081
LCG from AP	m	0.457
VCG from *keel*	m	0.067
τ_o	Degree (°)	1.0
β	Degree (°)	20
Δ	Kg	10.890
$I_{yy} = I_{zz}$	$Kg.m^2$	0.235

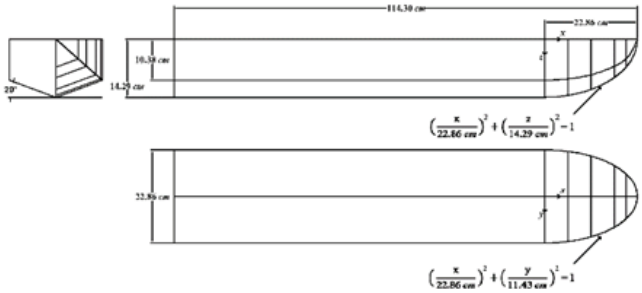

Figure 1. Fridsma Hull Form

According to Koh & Yasukawa [11], there are 3 types of ship operational waters, namely shallow waters with a ratio of water depth and draft H/T between 1.2 – 1.5, medium waters/medium H/T 1.5 – 19.3 and deep waters H/T > 19.3, as shown in Figure 2. In this study, several tests were carried out to determine the effect of differences in water depth on ship resistance with the parameters listed in Table 2.

Table 2. Variations in Water Depth

Parameter	Value
Shallow Water	1.4 H/T (0.1045 m)
Deep Water	20 H/T (1.5 m)

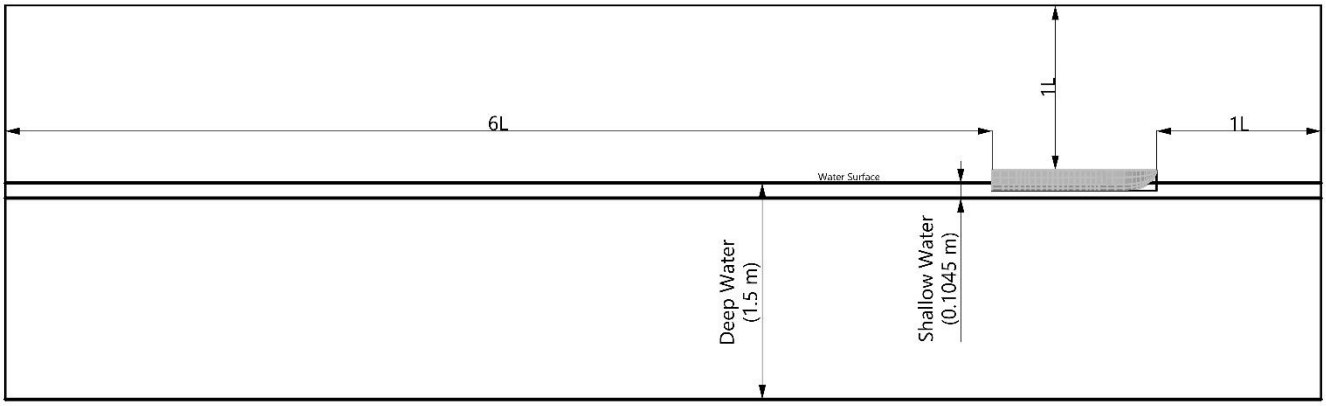

Figure 2. Visualization of Water Depth

2.2. Numerical Methods & Boundary Conditions

The numerical analysis used in this step is the Computational Fluid Dynamics method. The RANS (Reynolds-Averaged Navier-Stokes) equation is a method that represents the law of conversion of mass and momentum. The RANS equation is widely used in solving hydrodynamic problems with the incompressible flow with the equation:

$$\nabla . V = 0 \tag{1}$$

$$\rho \frac{\partial V}{\partial t} = -\nabla P + \mu \Delta V + \nabla . T_{Re} + S_M \tag{2}$$

Where ∇ is volume, V is average velocity vector, ρ is density, t is time, P is average compression area, μ is dynamic viscosity, T_{Re} is tensor of Reynolds stress, Δ is displacement and S_M is source vector momentum.

Two methods are most efficient in solving numerical simulations, namely morphing mesh and overset. This study uses the morphing mesh method because this method is more efficient from a computational point of view. This method allows the mesh to move around the hull without losing the physical continuity where the hull has a dynamic interaction with the fluid. Making a virtual towing tank is divided into two geometries based on the overset mesh method, namely background as a donor and overset as an acceptor [12]. The dimensions used in this study are listed in Table 3 and Figure 3 as a visualization of towing tank. Details boundary conditions can be seen in Table 4.

Table 3. Towing Tank Dimension

Parameter	*Background*
Length (m)	2L from FP
	6L from AP
Height (m)	1L from *deck*
	3L from *keel*
Width (m)	1.25L from *symmetry*

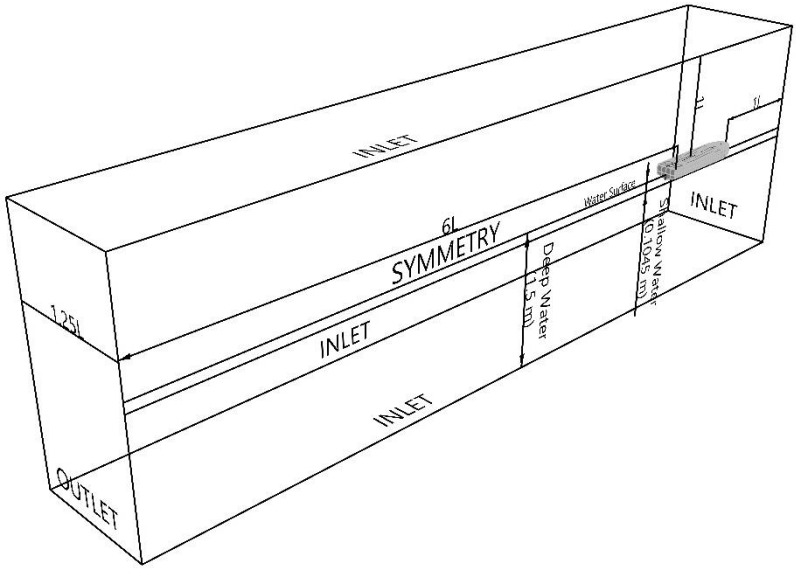

Figure 3. Visualization of Towing Tank

Wall function (y+) is a dividing wall between the wall (wall) and fluid flow which is used to improve calculation accuracy. The research by Avci et. al. used a y+ value between 45 – 60 for more accurate results [13]. The calculation of the y+ value according to ITTC is stated in the equation below [14] :

$$\frac{y}{L} = \frac{y^+}{R_e\sqrt{\frac{C_f}{2}}} \tag{3}$$

Time-step is the time interval for each iteration calculation in a numerical simulation. The smaller the time step, the more accurate the results will be. In CFD calculations, determining the time step with the ship's speed. The faster the ship, the smaller the time step used. The time step used in this study is 0.005 seconds. This refers to ITTC recommendations [13] contained in equation 4. Where L is the length of the ship and U is the speed of the ship.

$$\Delta t \text{ ITTC} = 0.005 \sim 0.01 \frac{L}{U} \tag{4}$$

Table 4. Boundary Conditions

Parts	Boundary Conditions	Type
Ship Hull	Wall	Six DOF Body
Outlet	Pressure Outlet	Hydrostatic Pressure
Symmetry Plane	Symmetry	Symmetry Plane
Bottom	Velocity Inlet	The velocity of Flat Vof Waves
Inlet	Velocity Inlet	The velocity of Flat Vof Waves
Top	Velocity Inlet	The velocity of Flat Vof Waves

2.3. Grid Study

Mesh studies are carried out to find the most suitable mesh for the simulation to be carried out [15]. In this study, 5 grid variations were used (Table 5). The results of the study using the bare hull model at a speed of Fn 1.2. When the number of cells/mesh used is less, the predicted values for all parameters will be different [16].

Table 5. Cell Size and Count in Million (M)

No. Grid	Minimum Cell Size (Δ x/B)	Cell Count
1	0.06	0.58 M
2	0.055	0.7 M
3	0.05	0.85 M
4	0.045	1.05 M
5	0.04	1.38 M

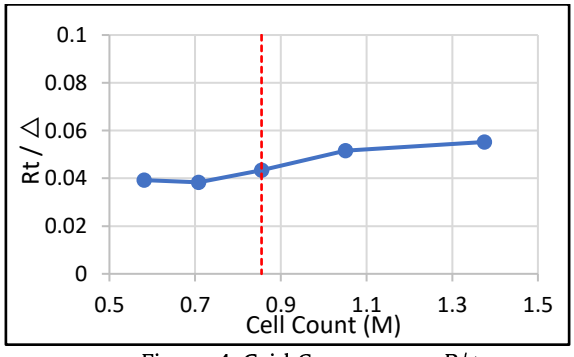

Figure 4. Grid Convergence R/Δ

Figures 4 and 5 are graphs of the resistance values and trim angles of each sample grid. Resistance is described with non-dimensional units R/Δ , R as the symbol for the resistance value and Δ as the symbol for the ship's displacement/volume. For trim angles described with angle units (°).

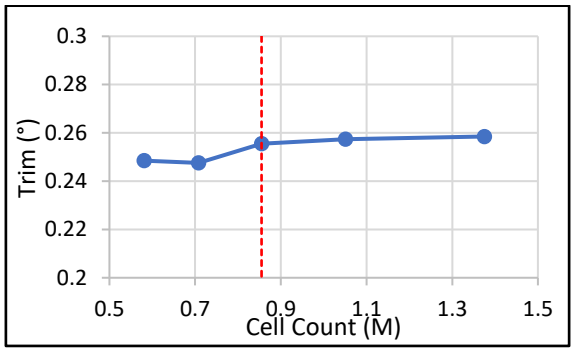

Figure 5. Grid Convergence Trim

Figure 4, shows that the more cells/mesh the higher the resistance value. Figure 5 shows the rise and fall of the results of the trim values for each grid used. As the number of cells increases, the data values converge. Convergence in the data is found in grid number 3. The blue line on the graph shows the convergence limit. The results from grids 4 and 5 are convergent, but it will take a long time to simulate because the number of cells is also increasing. In this study, the authors use grid number 3 to carry out the simulation.

2.4. Validation

Validation was carried out on the results of numerical simulations using Fridsma's experimental data with a value of L/B = 5 and LCG = 0.6 L from AP. 5 speeds were used based on the Froude Number in Fridsma's experiment, namely 0.6, 0.9, 1.2, 1.5 and 1.8. Meshing is concentrated on the water surface and the hull is divided into two parts, namely the bottom, and hull to get more accurate results.

From the following Figure 6, the Y axis is a non-dimensional unit of resistance expressed by R/Δ , with Newton as the unit of resistance (R) and Kilogram as the unit of displacement (Δ). While the X axis is a non-dimensional unit of speed expressed in the Froude Number.

From Figure 6. (a), it can be seen that all charts have the same trend. But at the Fn speed of 0.9 – 1.8,

it shows that the resistance value from the Fridsma experiment is smaller than the results of numerical calculations. The inaccuracy of the simulation results also occurs in Wheeler et al who explained that the inaccuracy of the simulation results could be caused by differences in the location of the ship's center of gravity, which would affect the drag and trim results if it shifted even a little [17].

From Figure 6. (b), the numerical calculation graph shows the pattern of trim results resembling Fridsma's experimental results. Therefore, these results can be used as a reference in comparing the several variations that will be used in this study.

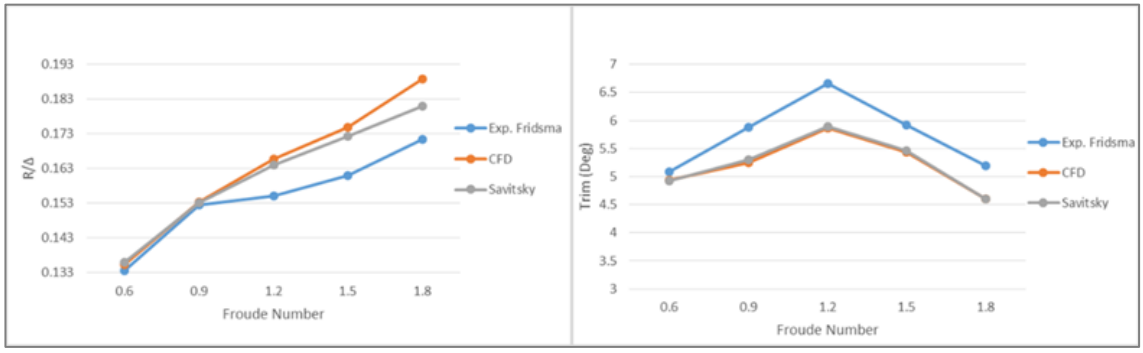

(a) (b)

Figure 6. Validation (a) R/Δ , (b) Trim

3. Results and Discussion

In this study, a Fridsma Hull simulation was carried out to determine the drag performance in shallow and deep waters. There are 2 components of the total resistance studied in this study, namely shear drag and pressure drag.

3.1. Characteristics of Fridsma Hull Resistance to Differences in Depth Levels

The results of the prediction of total resistance with pressure drag and shear drag as components using CFD software at each speed in deep and shallow waters can be seen in Figure 7. (a-c). This research was conducted in deep waters with a H/T ratio of 20 (1.5 m) and shallow waters with a H/T ratio of 1.4 (0.1045 m). In the graph containing the results of the prediction of the drag obtained from the CFD simulation, the resistance is expressed in non-dimensional units R/Δ , with R as the resistance and Δ as the displacement or weight of the ship. The results of the prediction of resistance are expressed in each non-dimensional unit for speed, namely the Froude Number.

Figure 7. (a) shows the results of pressure drag in deep waters are lower than in shallow waters. For shear drag decreased at Fn 1.5 in shallow waters. The total resistance in Figure 7. (c) shows an increase in shallow waters when compared to deep waters.

This is caused by a decrease in external pressure along the bottom of the ship's hull which interacts with the sea bed/sea floor and an increase in flow velocity between the bottom of the ship's hull and the bottom of the water which is called the squat phenomenon.

The Squat effect is a hydrodynamic phenomenon that occurs when ships operate in shallow waters so that when the ship travels at a certain speed it produces a low-pressure area under the hull and causes the hull to approach the bottom of the water. The squat phenomenon is caused by the flow of water that should flow under the hull encountering obstacles because the distance between the hull and the bottom of the water is too low. Based on Leonardo's law, the squat effect causes the water flow to move faster under the hull and refers to Bernoulli's theorem, an increase in water flow velocity causes a pressure drop under the hull causing the ship to be pulled to the bottom of the water. When a ship experiences a squat effect, the ship will experience bow trim or stern trim.

In high-speed planing vessels, trim is an important component because it affects the total drag and determines the location of stagnation lines in the hull. Trim is produced by a combination of propulsion moment, water pressure, drag, and lift. Figure 7. (d) shows an increase in trim at Fn 0.6 – 1.2 and a decrease at Fn 1.5 – 1.8 in each water.

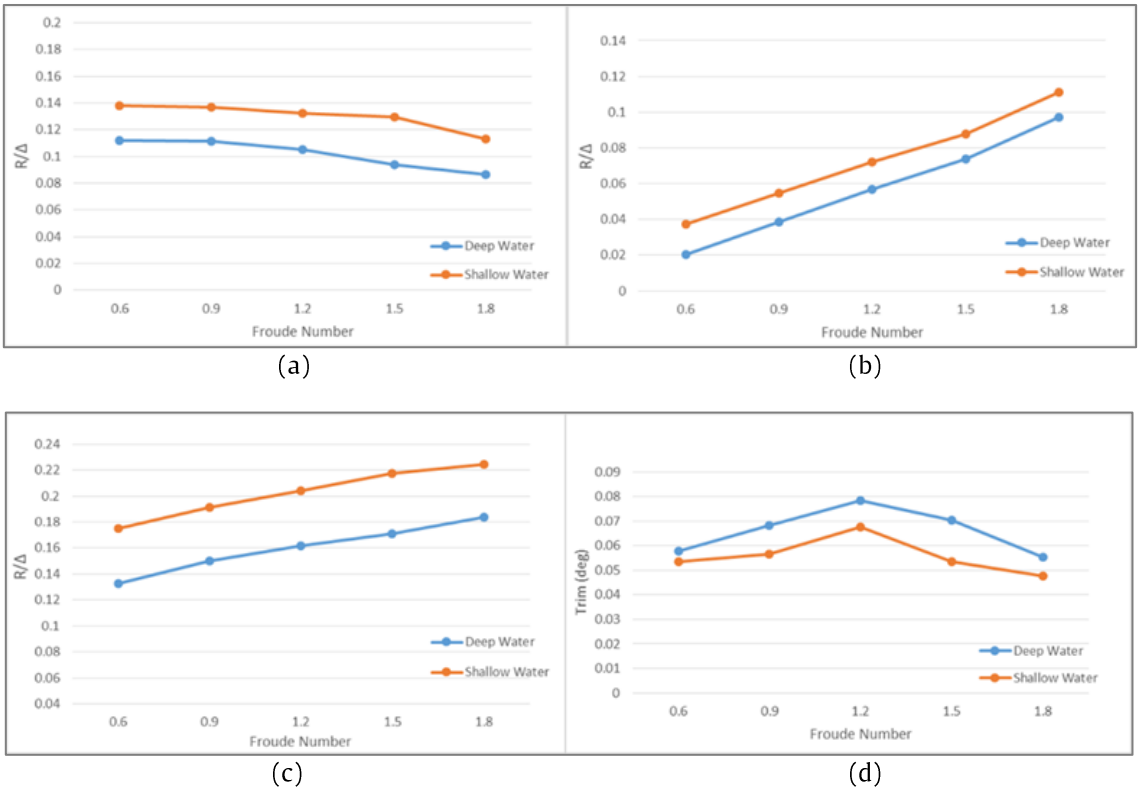

Figure 7. Comparison results value in each condition (a) pressure drag, (b) shear drag, (c) drag total, and (c) trim value.

3.2. Pressure Distribution at Bottom of The Hull

A comparison of pressure distribution at different speeds and the water level is shown in Figures 8 and 9. Significant pressure distribution changes occur at Fn 0.9 – 1.8, where the Fridsma hull form enters the hump region. The Hump region is the phase where the ship changes from the displacement phase to the planning phase.

At all speeds, the pressure develops from a maximum value at the stagnation line to a minimum value at which water separation occurs. Due to the separation of the streams, the relative pressure at the stern is negative and reaches its maximum value at the stagnation line where the water reattaches the hull. The image shows a pressure area where the water separates from the chine. The results of the comparison of the total resistance in shallow water in Figure 7 show the increase and decrease in resistance values. This is caused by a decrease in external forces along the bottom of the ship hull which interacts with the sea bed/sea floor and an increase in flow velocity between the bottom of the ship and the bottom of the water which is called the squat phenomenon [18] as shown in Figure 8. Figure 9 shows the pressure comparison in deep water, significant differences occur at high speeds at Fn 1.8.

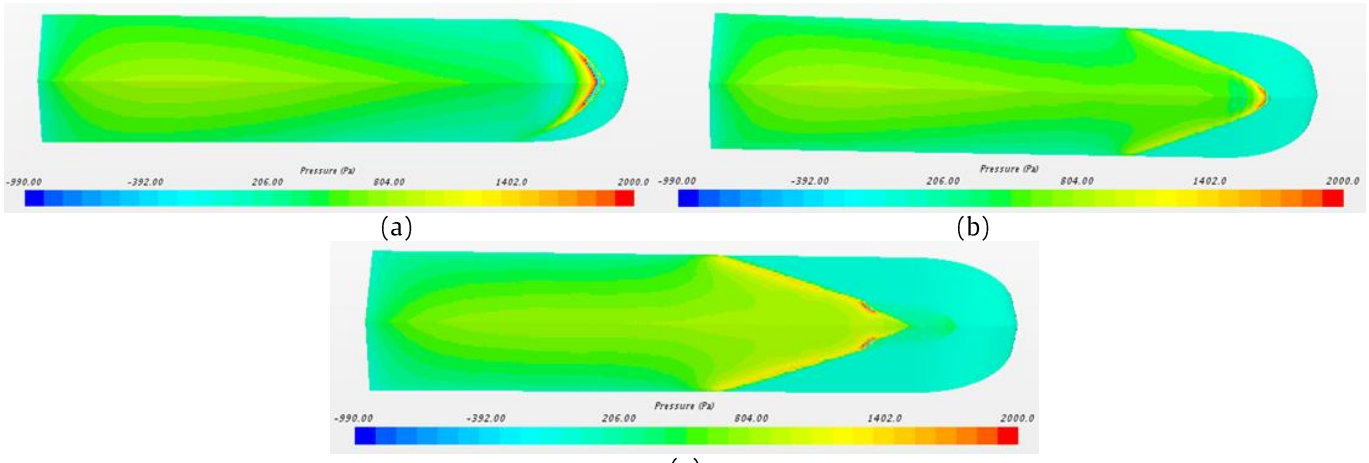

(a) (b)

(c)

Figure 8. Pressure distribution at shallow water (a) Fn 0.9, (b) Fn 1.2, and (c) Fn 1.8

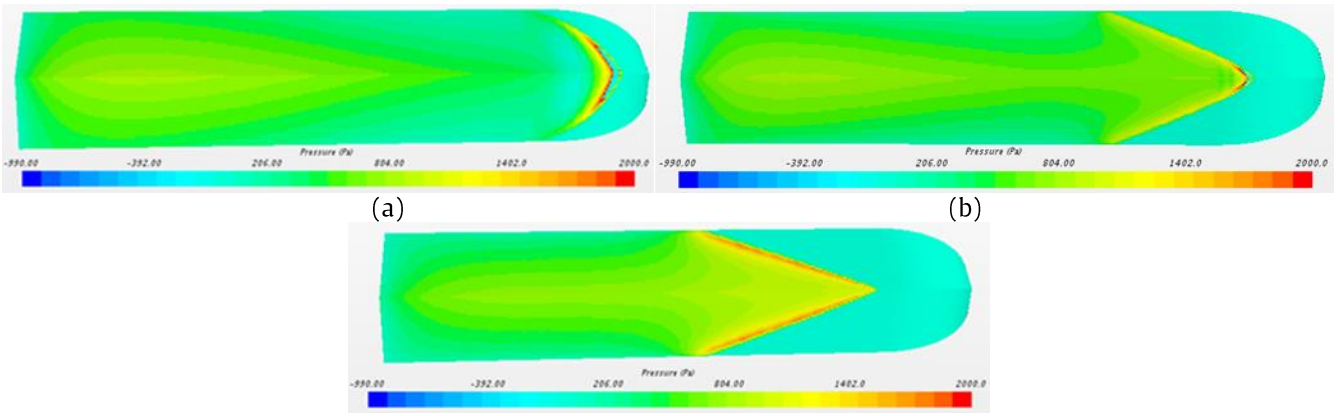

(a) (b)

(c)

Figure 9. Pressure distribution at deep water (a) Fn 0.9, (b) Fn 1.2, and (c) Fn 1.8

4. Conclusion

This study examines the comparison of resistance due to differences in the level of water surface depth on the performance of Fridsma hull. The CFD approach based on the finite volume method is used to examine the hydrodynamic characteristics of the planing hull at different speeds in deep and shallow waters. To validate the model used, a numerical calculation of the resistance was carried out with the available experimental data at 5 different speeds. Good compatibility has been shown from the results of this comparison. So that the CFD model in this study can be used to estimate the right resistance. The total resistance of Fridsma in shallow waters H/T 1.4 increased at each speed when compared to the total resistance in deep waters H/T 20. On average in deep waters, it can reduce the total resistance by around 22.34% compared to shallow waters.

Acknowledgment

This research was funded by Ministry of Education, Culture, Research, and Technology of Indonesia, grant number 187-06/UN7.6.1/PP/2022.

References

[1] G. Hou, B. Johnson, J. Degroff, S. Trenor, and J. Michaeli, " Dynamic response modeling of high-speed planing craft with enforced acceleration," *Ocean Engineering*, vol. 192, p. 106493, 2019, doi: 10.1016/j.oceaneng.2019.106493.

[2] D. J. Kim, S. Y. Kim, Y. J. You, K. P. Rhee, S. H. Kim, and Y. G. Kim, " Design of high-speed planing hulls for the improvement of resistance and seakeeping performance," *International Journal of Naval Architecture and Ocean Engineering*, vol. 5, no. 1, pp. 161– 177, 2013, doi: 10.2478/ijnaoe-2013-0124.

[3] S. Samuel, A. Trimulyono, and A. W. B. Santosa, " Simulasi CFD pada Kapal Planing Hull," *Kapal: Jurnal Ilmu Pengetahuan dan Teknologi Kelautan*, vol. 16, no. 3, pp. 123– 128, 2019, doi: 10.14710/kapal.v16i3.26397.

[4] W. W. K, " Design and Construction of High Speed, Hard Chine Planing Hull," *KDU Int. Res. Symp. Proc*, pp. 211–217, 2013.

[5] S. R. Lucas, J. C. Mcgowcm, R. S. Salzar, C. Planchak, J. E. Gelz, and J. Mcdevitt, " 2nd Chesapeake Power Boat Symposium 2010," *2nd Chesap. Power Boat Symp. 2010*, 2010.

[6] K. I. Matveev, " On application of three-dimensional linearized potential-flow model for shallow-water planing," *Journal of Ocean Engineering and Science*, vol. 3, no. 3, pp. 218– 222, 2018, doi: 10.1016/j.joes.2018.08.002.

[7] M. Terziev, T. Tezdogan, and A. Incecik, " Modelling the hydrodynamic effect of abrupt water depth changes on a

ship travelling in restricted waters using CFD," *Ships Offshore Structure*, vol. 16, no. 10, pp. 1087– 1103, 2021, doi: 10.1080/17445302.2020.1816731.

[8] A. De Marco, S. Mancini, S. Miranda, R. Scognamiglio, and L. Vitiello, " Experimental and numerical hydrodynamic analysis of a stepped planing hull," *Applied Ocean Research*, vol. 64, pp. 135– 154, 2017, doi: 10.1016/j.apor.2017.02.004.

[9] A. Dashtimanesh, A. Esfandiari, and S. Mancini, " Performance prediction of two-stepped planing hulls using morphing mesh approach," *Journal of Ship Production and Design*, vol. 34, no. 3, pp. 236– 248, 2018, doi: 10.5957/JSPD.160046.

[10] G. Fridsma, S. S. Command, and C. Station, " A Systematic Study of The Rough-water Performance of Planning Boat," 1969.

[11] K. K. Koh and H. Yasukawa, " Comparison study of a pusherbarge system in shallow water, medium shallow water and deep water conditions," *Ocean Engineering*, vol. 46, pp. 9– 17, 2012, doi: 10.1016/j.oceaneng.2012.03.002.

[12] Samuel, A. Trimulyono, P. Manik, and D. Chrismianto, " A numerical study of spray strips analysis on fridsma hull form," *Fluids*, vol. 6, no. 11, 2021, doi: 10.3390/fluids6110420.

[13] A. G. Avci and B. Barlas, " An experimental and numerical study of a high speed planing craft with full-scale validation," Journal of Marine Science and Technology, vol. 26, no. 5, pp. 617– 628, 2018, doi: 10.6119/JMST.201810_26(5).0001.

[14] ITTC, " Practical Guidelines for Ship CFD Applications," *ITTC – Recomm. Proced. Guidel. ITTC*, pp. 1– 8, 2011.

[15] A. Lungu, " A DES-based study of the flow around the self-propelled DARPA Suboff working in deep immersion and beneath the free-surface," *Ocean Engineering*, vol. 244, p. 110358, 2022, doi: 10.1016/j.oceaneng.2021.110358.

[16] A. Hosseini, S. Tavakoli, A. Dashtimanesh, P. K. Sahoo, and M. Kõrgesaar, " Performance Prediction of a Hard-Chine Planing Hull by Employing Different CFD Models," *Journal Marine Science and Engineering*, vol. 9, no. 5, 2021, doi: 10.3390/jmse9050481.

[17] M. P. Wheeler, K. I. Matveev, and T. Xing, " Validation study of compact planing hulls at pre-planing speeds," *Am. Soc. Mech. Eng. Fluids Eng. Div. FEDSM*, vol. 2, pp. 1– 8, 2018, doi: 10.1115/FEDSM2018-83091.

[18] K. Elsherbiny, T. Tezdogan, M. Kotb, A. Incecik, and S. Day, " Experimental analysis of the squat of ships advancing through the New Suez Canal," *Ocean Engineering*, vol. 178, pp. 331– 344, 2019, doi: 10.1016/j.oceaneng.2019.02.078.